

# Dynamic Analysis of Pelton Turbine and Assembly

Aman Rajak, Prateek Shrestha, Manoj Rijal, Bishal Pudasaini, Mahesh Chandra Luintel

Department of Mechanical Engineering, Central Campus, Pulchowk, Institute of Engineering, Tribhuvan University, Nepal

Corresponding Email: 067bme601@ioe.edu.np, 067bme627@ioe.edu.np, 067bme620@ioe.edu.np, mcluintel@ioe.edu.np

**Abstract:** In this study, dynamic analysis of the Pelton turbine and assembly is carried out to obtain the natural frequency of the system. A mathematical model is developed to calculate the kinetic energy and the strain energy. The equations of motion are derived using Lagrange equations and the Rayleigh-Ritz method is used to study the basic phenomena of cylindrical mode of rotor. For the validation purpose, modal analysis is carried out in Mechanical APDL 14.5 to obtain the critical frequency. The developed methodologies were followed to find the solution of the Pelton turbine test setup of National College of Engineering. The critical frequencies of the system were found to be 192.69 Hz and 192.73 Hz in the global X and Y direction for the cylindrical mode. The result from simulation was 137.86 Hz and 137.98 for the same type of system. Simulation works were further carried out considering the bearing stiffness. Sensitivity of various parameters decisive for dynamic behavior were investigated

**Keywords:** Pelton; natural frequency; dynamic analysis; Campbell diagram

## 1. Introduction

The study of dynamic behavior of hydraulic machinery has been of great importance in order to understand the operating mechanism and the failures associated with the machines. Machines are set to vibration under several excitation modes. So, accurate prediction of vibration characteristics is crucial in the design stage of hydraulic machinery considering the requirements of quality, performance and safety. In case of Pelton Turbine, the system can be assumed to a disk mounted on the shaft with bearings at its supports. This system, usually signified as Pelton Turbine and assembly, operates at high rotational speed for the purpose of electricity generation. So, there is a need to develop methodologies that allow for more realistic dynamic analysis of Pelton turbines because prototyping and testing cost are exceptionally high and failure is generally disastrous in the practical applications and testing of these systems.

Pelton Turbines has been widely used in hydro-electric plants around the country. Beside large hydro power plants, Pelton turbines are also being used in several micro hydro power plants. In MHP plants, the turbine is usually designed and manufactured by local manufacturers within the country. Several researches have been conducted in the field of sediment and erosion for improvement of designs. However, very less work has been done in the field of the dynamic behavior of turbines and their effects in design and operation. Even though this is a well-established turbine technology, there are many unanswered questions regarding design and optimization. Thus, further development is still relevant today. This work of dynamic analysis of Pelton turbine identifies the assembly as a rotor disk system as shown in Figure

1 and hence dynamic behaviour is studied by developing a mathematical model for rotor disk system.

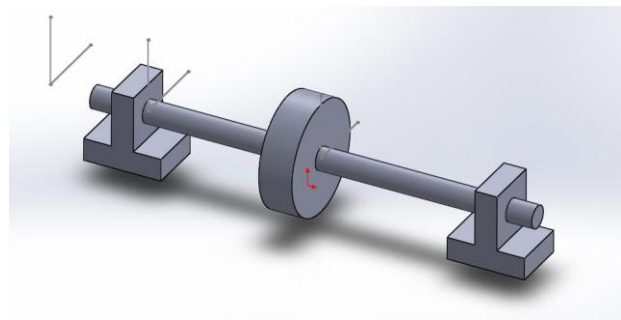


Figure 1: Simple Rotor Disk System

## 2. Literature Review

Rotor dynamics fundamental:

Rotor dynamics is a specialized branch of applied mechanics concerned with the behavior and diagnosis of rotating structures such as turbines, engines and computer disk storage. Rotor dynamics can be divided into three different types of motion, lateral, longitudinal and torsional. Lateral is also called bend rotor dynamics and is associated with bending of the rotor. Torsional is the modes when the rotor is twisting around its own axis. Longitudinal modes are when the rotor parts are moving in axial direction (Samuelsson, 2009).

A simple approach to rotor dynamics study is often attributed to the Jeffcott rotor model. The model consists of a single disk centrally located on a circular shaft considered with damping. Many variations of Jeffcott rotor have been studied but its most frequent features are a single, rigid disk mounted on a circular,

flexible shaft, which is supported by bearings at each end.

The dynamic behavior of flexible rotor systems subjected to base excitation (support movements) is investigated theoretically and experimentally in the paper by (Duchemin et al., 2006). The paper has developed a mathematical model for total energy of the system and the equation of motion has been derived using energy method. The study focuses in bending near the critical speeds of rotation.

In the research paper (Hsieh et al., 2006), a modified transfer matrix method for the coupling lateral and torsional vibrations of symmetric rotor-bearing systems have been used. Euler's angles are used to describe the orientations of the shaft element and disk and several numerical examples are presented to demonstrate the applicability of this approach.

A similar approach has been used in the developing the mathematical model for energy and then the equation of motion of the multi-rotor system in the dissertation work (Paulo, 2011) with aid of Euler's angle orientation and Lagrange's equation of motion.

### 3. Development of the mathematical model

The basic elements considered for developing the mathematical model are the shaft, the disks and the mass unbalance. The complete mathematical model has been developed in three phases. The equation of motion for the system has been derived using energy method.

- Derivation of total energy of the system
- Derivation of equations of motion
- Solution of EOM to find the expression of natural frequency and responses

#### 3.1 Phase I – Total Energy of the system

For the disk, shaft and mass unbalance kinetic energy  $T$  must be computed and in case of the shaft, strain energy is calculated, since it is the only flexible component considered. The bearings are considered to be rigid and undamped.

Three reference frames are used.

$x_d y_d z_d$  = fixed on the disk center

$x_s y_s z_s$  = fixed with shaft

$X Y Z$  = fixed inertial frame

### The Disk

The disk is considered rigid. Thus, kinetic energy is the only energy characterizing the component. The coordinate of disk center 'D' is  $u(z, t)$ ,  $v(z, t)$  and  $z$  with reference to inertial frame  $XYZ$  coordinate system. Then, the position vector of the disk center 'D' in the  $XYZ$  coordinate system can be written in the form

$$\vec{R} = \begin{Bmatrix} u \\ v \\ z \end{Bmatrix} \quad (1)$$

The orientation of the rotating element in three dimensional motions can be completely described using Euler's angles defined via three successive rotations to specify the relations between the principal axes of the rotating frame and the fixed frame.

The rotating sequence for defining Euler's angle is done by following order

- a) Rotating the frame fixed with the disk center by angle  $\phi$  about Y-axis
- b) Rotating the intermediate axis by angle  $\theta$  about  $x_1$  axis
- c) Finally, rotating another intermediate axis by angle  $\psi$  about  $z_2$  axis.

Through the coordinate transformation, the components of the angular velocities in the directions of principal axes can be found to be

$$\therefore \begin{bmatrix} \omega_x \\ \omega_y \\ \omega_z \end{bmatrix} = \begin{bmatrix} \cos(\psi) \dot{\theta} + \cos(\theta) \sin(\psi) \dot{\phi} \\ -\sin(\psi) \dot{\theta} + \cos(\theta) \cos(\psi) \dot{\phi} \\ -\sin(\theta) \dot{\phi} + \dot{\psi} \end{bmatrix} \\ = \begin{bmatrix} \cos(\psi) \dot{\theta} + \sin(\psi) \dot{\phi} \\ -\sin(\psi) \dot{\theta} + \cos(\psi) \dot{\phi} \\ -\dot{\phi} \theta + \dot{\psi} \end{bmatrix} \quad (2)$$

Where,  $\theta$ ,  $\phi$  and  $\psi$  are Euler's angle and  $\dot{\theta}$ ,  $\dot{\phi}$  and  $\dot{\psi}$  are the rate of nutation, rate of precession and rate of spin respectively. We can assume  $\cos(\theta) \approx 1$ ,  $\cos(\phi) \approx 1$ ,  $\sin(\theta) \approx \theta$  and  $\sin(\phi) \approx \phi$

The kinetic energy of the disk is given by

$$T_D = \frac{1}{2} M_D (\dot{u}^2 + \dot{v}^2) + \frac{1}{2} (I_{Dxx} \omega_x^2 + I_{Dyy} \omega_y^2 + I_{Dzz} \omega_z^2) \quad (3)$$

Where,  $M_D$  is the mass of the disk and  $I_{Dxx}$ ,  $I_{Dyy}$  and  $I_{Dzz}$  are the moment of inertia about the principal axis  $XYZ$  principal axis  $XYZ$ . Since the disk is assumed to be symmetric,  $I_{Dxx} = I_{Dyy}$ .

$$\therefore T_D = \frac{1}{2} M_D (\dot{u}^2 + \dot{v}^2) + \frac{1}{2} I_{Dxx} [\dot{\theta}^2 + \dot{\phi}^2] + \frac{1}{2} I_{Dzz} (-2\dot{\phi}\dot{\psi}\theta + \dot{\psi}^2) \quad (4)$$

### The Shaft

The shaft is considered as a flexible element having a constant cross-sectional area. Thus, it has both kinetic and strain energies. The kinetic energy of the shaft is defined similar to the disk but is defined for an element and integrated over the length of the shaft 'L'.

The kinetic energy of the shaft is:

$$T_S = \frac{\rho S}{2} \int_0^L (\dot{u}^2 + \dot{v}^2) dz + \frac{\rho I_{xx}}{2} \int_0^L \omega_x^2 dz + \frac{\rho I_{yy}}{2} \int_0^L \omega_y^2 dz + \frac{\rho I_{zz}}{2} \int_0^L \omega_z^2 dz$$

$$\therefore T_S = \frac{\rho S}{2} \int_0^L (\dot{u}^2 + \dot{v}^2) dz + \frac{\rho I}{2} \int_0^L (\dot{\theta}^2 + \dot{\phi}^2) dz + \rho I L \omega^2 - 2\rho I \dot{\psi} \int_0^L \theta \dot{\phi} dz \quad (5)$$

Where,  $\rho$  denotes mass per unit volume,  $S$  is the shaft's cross-sectional area which is assumed constant throughout the length, and  $I$  is the second moment of inertia of the shaft cross-section about its neutral axis.

Potential Energy of the shaft:

Considering the strain caused by the rotation of the shaft, the strain energy of the shaft is given by

$$U_S = \frac{EI}{2} \int_0^L \left[ \left( \frac{d^2 u}{dz^2} \right)^2 + \left( \frac{d^2 v}{dz^2} \right)^2 \right] dz \quad (6)$$

The bearing at the support is assumed to be rigid described by high elastic stiffness and negligible damping.

The expression for the total kinetic energy of the system is:

$$T = T_D + T_S$$

$$T = \frac{1}{2} \left\{ M_D (\dot{u}^2 + \dot{v}^2) + \frac{1}{2} I_{Dxx} (\dot{\theta}^2 + \dot{\phi}^2) + \frac{1}{2} I_{Dzz} (\dot{\psi}^2 - 2\dot{\psi}\dot{\phi}\theta) \right\} + \left\{ \frac{\rho S}{2} \int_0^L (\dot{u}^2 + \dot{v}^2) dz + \frac{\rho I_{Sxx}}{2} \int_0^L (\dot{\theta}^2 + \dot{\phi}^2) dz + \rho I_{Sxx} L \omega^2 - 2\rho I_{Sxx} \dot{\psi} \int_0^L \theta \dot{\phi} dz \right\} \quad (7)$$

The potential energy of the system is

$$U_E = \frac{EI}{2} \int_0^L \left[ \left( \frac{d^2 u}{dz^2} \right)^2 + \left( \frac{d^2 v}{dz^2} \right)^2 \right] dz \quad (8)$$

### 3.2 Phase II – Equation of motion

Now for the first mode assuming the displacement function as:

$$f(z) = \sin\left(\frac{\pi z}{L}\right) \quad (9)$$

The displacements in the x and y direction for a current point are expressed as

$$u(z, t) = f(z) \cdot U(t) = U \cdot \sin\left(\frac{\pi z}{L}\right)$$

$$v(z, t) = f(z) \cdot V(t) = V \cdot \sin\left(\frac{\pi z}{L}\right) \quad (10)$$

Also, as angular displacements  $\phi$  and  $\theta$  are small, they are approximated as

$$\theta = \frac{\partial v}{\partial z} = g(z) \cdot V(t) = \frac{\pi}{L} V \cdot \cos\left(\frac{\pi z}{L}\right)$$

$$\phi = -\frac{\partial u}{\partial z} = -g(z) \cdot U(t) = -\frac{\pi}{L} U \cdot \cos\left(\frac{\pi z}{L}\right) \quad (11)$$

Applying above expressions in the kinetic energy, it results:

$$T = \frac{1}{2} m (\dot{U}^2 + \dot{V}^2) + \omega \cdot a \cdot \dot{U} \cdot V + \left( \frac{1}{2} I_{Dzz} \omega^2 + \rho I_{Sxx} L \omega^2 \right) \quad (12)$$

With the disk situated at middle of the shaft and applying the displacement function:

$$m = M_D + \frac{\rho S L}{2} + \frac{\rho I \pi^2}{2L} \quad (13)$$

$$a = \frac{\rho I_{Sxx} \pi^2}{L}$$

The potential energy comes out to be

$$U_E = \frac{\pi^4 E I_{Szz} (U^2 + V^2)}{4 L^3} \quad (14)$$

Using Lagrange equation in the above obtained kinetic and potential energy choosing generalized co-ordinates as  $U$  and  $V$ , we get equation of motion as:

$$\begin{bmatrix} m & 0 \\ 0 & m \end{bmatrix} \begin{Bmatrix} \ddot{U} \\ \ddot{V} \end{Bmatrix} + \omega \begin{bmatrix} 0 & a \\ -a & 0 \end{bmatrix} \begin{Bmatrix} \dot{U} \\ \dot{V} \end{Bmatrix} + \begin{bmatrix} K & 0 \\ 0 & K \end{bmatrix} \begin{Bmatrix} U \\ V \end{Bmatrix} = 0 \quad (15)$$

K is given by the relation as follows

$$K = \frac{\pi^4 EI}{2L^3} \quad (16)$$

### 3.3 Phase III - Analytical solution of the system

The equation of motion can be written as:

$$\begin{aligned} m\ddot{U} + a\omega\dot{V} + KU &= 0 \\ m\ddot{V} - a\omega\dot{U} + KV &= 0 \end{aligned} \quad (17)$$

These are two coupled linear differential equations of second order and their solution may be of the form

$$\begin{aligned} U &= \bar{U}e^{st} \\ V &= \bar{V}e^{st} \end{aligned} \quad (18)$$

Substituting U and V in the equation of motions and solving for s we get

$$s^2 = \frac{-(2mK + a^2\omega^2) \pm \sqrt{4mka^2\omega^2 + a^4\omega^4}}{2m^2} \quad (19)$$

The solution of the expression leads to two pairs of complex conjugate roots. The real part of the complex conjugate roots represents the rate of decay of the vibration and is given by,  $r_a = -\frac{\zeta_a\omega_a}{\sqrt{1-\zeta_a^2}}$ , where  $\zeta_a$  is called the viscous damping factor for mode 'a' and the imaginary part represents the corresponding natural frequency. Due to our assumption of undamped system the rate of decay of vibration is 0 in the solution.

## 4. Result and Analysis

The derived mathematical model is verified using the data of Pelton turbine test rig of National College of Engineering and for comparison simulation work is further carried out.

### 4.1 Pelton Turbine Model

The Pelton turbine installed at National College of Engineering by D-Matrix Engineering Services is taken as a case. A Pelton turbine model is developed in Solidworks 2013 for a jet diameter of 25mm as shown in the Figure below

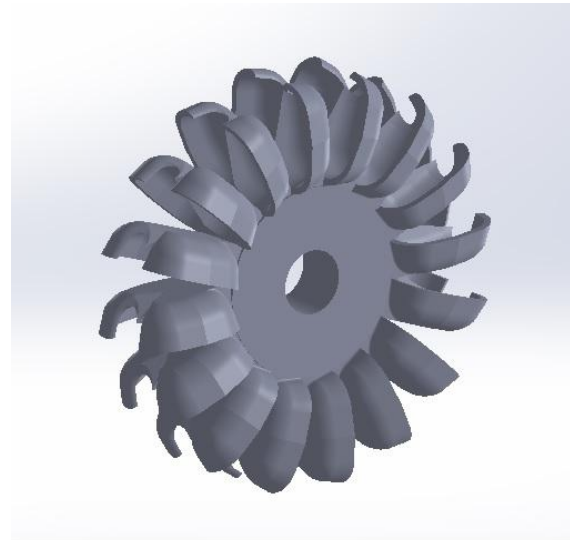


Figure 2: Pelton Turbine Model

The extracted parameters which are then used for further calculation of natural frequency are given below:

Mass of runner,  $M_D = 11.14$  kg

mass moment of inertia of disc along x-axis,

$$I_{Dxx} = 30.33 \times 10^{-3} \text{ kgm}^2$$

mass moment of inertia of disc along y-axis,

$$I_{Dyy} = 30.33 \times 10^{-3} \text{ kgm}^2$$

mass moment of inertia of disc along z-axis,

$$I_{Dzz} = 55.09 \times 10^{-3} \text{ kgm}^2$$

### 4.2 Analytical solution

The solution for natural frequency of the system is obtained from the equation (19).

Now substituting the value of the parameter as provided from NCE model in a, k and m.

Table 1: Parameters used in calculation of critical frequency

Parameters	Value
Mass of runner, $M_D$ (kg)	11.14
cross sectional area of shaft, S ( $\text{m}^2$ )	$1.25 \times 10^{-3}$
density of shaft material, $\rho$ ( $\text{kg}/\text{m}^3$ )	7850.00
length of shaft, L (mm)	497.00
$I_{xx}$ ( $\text{m}^4$ )	$1.256 \times 10^{-7}$
$I_{szz}$ ( $\text{m}^4$ )	$2.513 \times 10^{-7}$
E ( $\text{N}/\text{m}^2$ )	$2 \times 10^{11}$
Spin speed, $\omega$ (rad/s)	157.07

Then we have,

$$s_1 = 0 + 1210.8i \text{ and } s_2 = 0 + 1211.0i$$

Hence, the natural frequencies are

$$\omega_1 = \frac{1210.8}{2\pi} = 192.69 \text{ Hz}$$

$$\omega_2 = \frac{1211.0}{2\pi} = 192.73 \text{ Hz}$$

The natural frequency of the system along the respective degree of freedom U and V were found to be 192.69 Hz and 192.73 Hz respectively.

The Campbell diagram plot using the mathematical model as represented in the figure below.

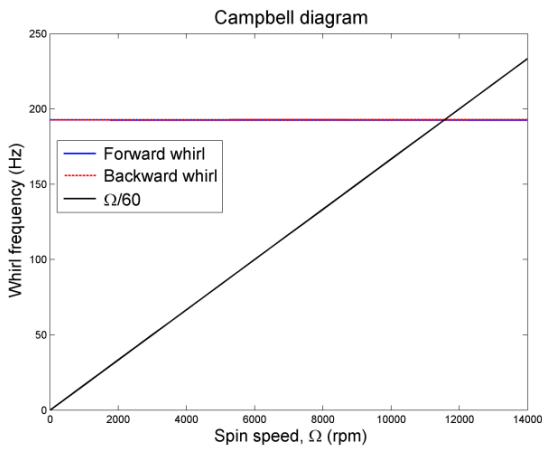


Figure 3: Campbell Diagram

### 4.3 Simulation result

The model using the similar geometric parameters of the above mentioned Pelton Turbine was made and the corresponding material properties and real constants were fetched in the model. The model of the shaft, made using BEAM188 element was meshed with 497 elements, with edge length of 1 mm and boundary conditions of a simply-supported beam were given. For subjecting the mass of Pelton runner MASS21 element was defined.

Using the above given data the simulation results, the natural frequencies of the system for the cylindrical mode was found to be 137.86 Hz and 137.98 Hz.

The Campbell plot for the assembly was found as shown in figure 3.

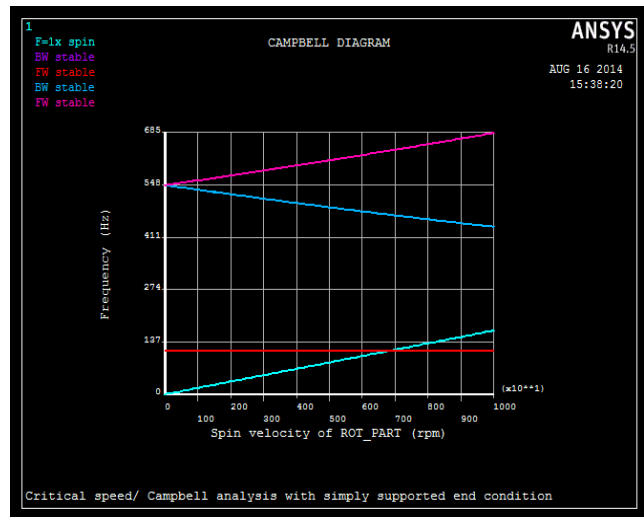


Figure 4: Campbell Diagram with rigid support

But in actual rotor dynamics, bearing support is the essential, hence the bearing stiffness is to be considered. Considering this, simulation of the assembly using bearing stiffness was done. The bearing element was defined using COMBI214.

Using the bearing element the natural frequencies of the system for the cylindrical mode were found to be 137.72 Hz and 137.93 Hz.

The Campbell plot for the assembly considering the spring element was found as:

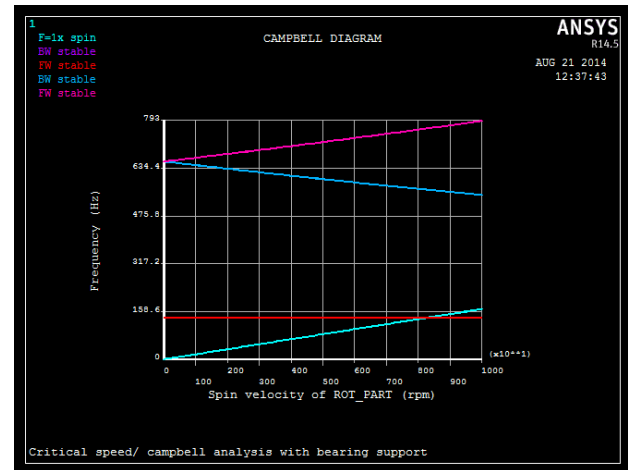


Figure 5: Campbell Diagram with consideration of bearing stiffness

### 4.4 Sensitivity of various parameters on dynamic response of the system

With the aid of the developed model, we analysed various decisive parameters effect and their sensitiveness in the natural frequency of the system.

Simulation works were also carried out to determine natural frequency at the varied parameters.

#### 4.4.1 Variation of natural frequency of the system with change in length of the shaft

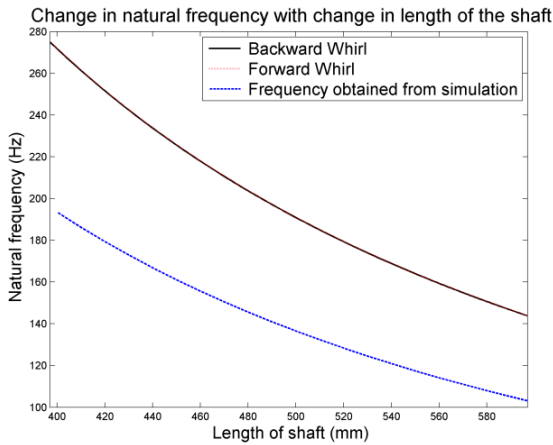


Figure 6: Variation of natural frequency with change in length of shaft

From equation (16), we can see that the stiffness is inversely proportional to  $L^3$  where  $L$  is the length of shaft. The plot shows that the frequency of the system decreases with increase in the shaft length.

#### 4.4.2 Variation of natural frequency of the system with change in diameter of the shaft

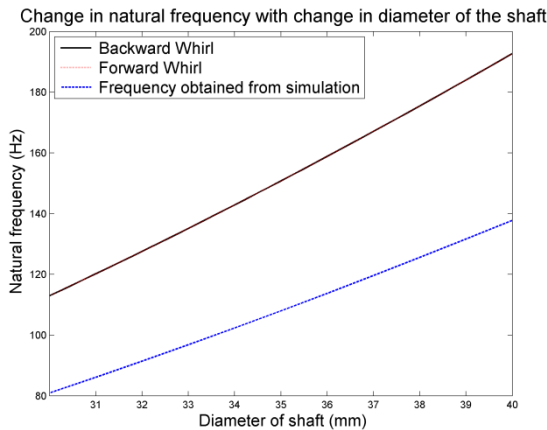


Figure 7: Variation of natural frequency with change in diameter of shaft

With the increase in diameter, the stiffness of the shaft also increases and hence the natural frequency also increases. The plot shows the variation obtained from both simulation and analytical solution.

#### 4.4.3 Variation of natural frequency of the system with change in stiffness of the bearing (simulation only)

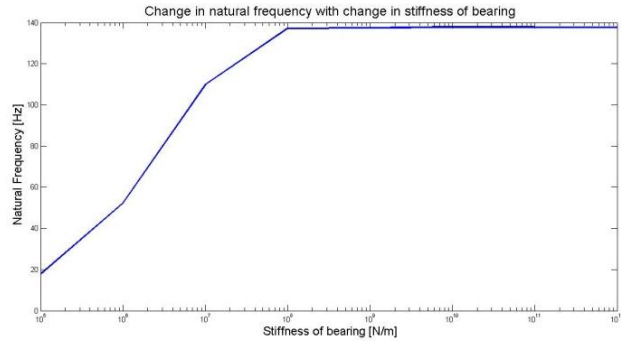


Figure 8: Simulation result of variation of natural frequency with change in stiffness of bearing

The frequency was found to decrease dramatically with decrease in the bearing stiffness (i.e. increase in the clearance between shaft and bearing) and can reach within the operating range.

## 5. Conclusion

This paper presented the methodologies to study the dynamic behavior of Pelton Turbine and assembly as a general shaft disk system. The mathematical model for dynamic behavior of the Pelton turbine assembly was thus formulated and the analytical solution of natural frequency was performed. The analytical results for a Pelton turbine laboratory setup shows that the natural frequency of the system lies in a good safe range. This also indicates that the contemporary design procedure followed by the manufacturers is reliable considering the dynamic behavior of the system. The analytical solution and the simulation results were found to be in fair agreement. The yielded result from the two approaches also supports the fact that the solution provided by Rayleigh-Ritz analytical solution is greater than the simulation results.

Furthermore the natural frequency of the system for the cylindrical mode i.e. fundamental mode was found to be less effected by gyroscopic effect as seen in the Campbell diagram. The major reason behind this is the position of the disk that was selected to derive the mathematical model.

Length of shaft and diameter of shaft has been found to be very sensitive parameters in determining the dynamic behavior of the system. Also stiffness of the bearing is a defining factor in a real system as seen from the simulation work. Stiffness of the bearing is a function of time and as bearing clearance increases, the stiffness decreases and could cause a critical vibration

problems decreasing the natural frequency to an unsafe limit after operation for certain period as seen from the sensitivity analysis.

## References

---

- (n.d.). Retrieved May 24, 2013, from <http://en.wikipedia.org/wiki/Rotordynamics>
- Beer, F. P., Johnston, E. R., DeWolf, J. T., & Mazurek, D. F. (2012). *Mechanics of Materials* (Sixth ed.). New York: The McGraw-Hill Companies, Inc.
- Duchemin, M., Berlioz, A., & Ferraris, G. (2006). Dynamic Behavior and Stability of a Rotor Under Base Excitation. *Journal of Vibration and Acoustics*, 128.
- Furnes, K. (2013). *Flow in Pelton Turbines*. Norwegian University of Science and Technology, Department of Energy and Process Engineering.
- Hsieh, S.-C., Chen, J.-H., & Lee, A.-C. (2006). A modified transfer matrix method for the coupling lateral and torsional vibrations of symmetric rotor-bearing systems. 289.
- Inc., A. *Ansys Help 14.5*.
- Inc., A. (2012). *ANSYS Inc. PDF Documentation for Release 14.5*.
- Kelly, S. G. (2012). *Mechanical Vibrations Theory and Applications* (SI ed.). Stamford, ST 06902: Cengage Learning.
- Lal, J. (1997). *Hydraulic Machinery*. Delhi: Metropolitan Book Company.
- Paulo, P. V. (2011). *A time-domain methodology for rotor dynamics: analysis and force identification*. Dissertation, Instituto Superior Tecnico, Universidade Tecnica de Lisboa.
- Samuelsson, J. (2009). *Rotor dynamic analysis of 3D-modeled gas turbine rotor in ANSYS*. Thesis, Department of Management and Engineering, Linköping's university.
- Sapkota, D., Thapa, R., & Poudel, S. P. (2006). *Study of Design and Development of Test Rig for Sand Erosion in Pelton Bucket*. Department of Mechanical Engineering, Pulchowk Campus, Institute of Engineering.
- Thomson, W. (1993). *Theory of Vibration with Applications*. New Jersey: A Simon and Schuster Company.
- Wikimedia Foundation, Inc. (2012). Retrieved March 27, 2014, from [http://en.wikipedia.org/wiki/Campbell\\_diagram](http://en.wikipedia.org/wiki/Campbell_diagram)